Aalto University

Gasparinetti, S.; Martinez-Pérez, M.J.; de Franceschi, S.; Pekola, J.P.; Giazotto, F.

Nongalvanic thermometry for ultracold two-dimensional electron domains

Nongalvanic thermometry for ultracold two-dimensional electron domains

S. Gasparinetti' , M. J. Martínez-Pérez, S. de Franceschi, J. P. Pekola, and F. Giazotto

Nongalvanic thermometry for ultracold two-dimensional electron domains

S. Gasparinetti,[1,a] M. J. Martínez-Pérez,[2] S. de Franceschi,[3] J. P. Pekola,[1] and F. Giazotto[2]

[1]*Low Temperature Laboratory, Aalto University, P.O. Box 15100, FI-00076 Aalto, Finland*
[2]*NEST Istituto Nanoscienze-CNR and Scuola Normale Superiore, I-56127 Pisa, Italy*
[3]*SPSMS, CEA-INAC/UJF-Grenoble 1, 17 Rue des Martyrs, F-38054 Grenoble Cedex 9, France*

Measuring the temperature of a two-dimensional electron gas at temperatures of a few mK is a challenging issue, which standard thermometry schemes may fail to tackle. We propose and analyze a nongalvanic thermometer, based on a quantum point contact and quantum dot, which delivers virtually no power to the electron system to be measured. © 2012 American Institute of Physics. [http://dx.doi.org/10.1063/1.4729388]

The availability of high-mobility two-dimensional electron gases (2DEGs), combined with the ability to cool them down to low temperatures, has led to the discovery of outstanding physical phenomena, such as the quantum Hall effect.[1] Refrigeration schemes are currently under investigation to cool the 2DEG below the conventional operating temperature of a dilution fridge (around 20 mK), down to 1 mK or below.[2,3] This achievement would open the way to a range of experiments of fundamental relevance and to a number of applications: electron interferometry,[4] study of correlated phases[5] and exotic effects,[6] charge pumping,[7] quantum computing,[8,9] and so on.

Several different types of electron thermometers have been proposed and realized.[10] However, as the temperature of electrons gets down to the mK range and below, finding a proper way to measure it in a non-invasive way becomes a critical issue. With the coupling between electrons and phonons becoming weaker and weaker, the power load that a micrometer-sized electron domain can sustain without overheating shrinks down to a few aW or less. In this regime, detection schemes based on transport measurements, such as the "conventional" quantum dot thermometer (QDT), become impractical as they inject high-energy quasiparticles which heat the system up, when not bringing it out of thermal equilibrium.

In this letter, we propose nongalvanic thermometry for 2DEGs. Here, nongalvanic refers to the absence of current transport between the measured electron system and the thermometer leads. We start with a quick review of the QDT. Then, we introduce its nongalvanic counterpart, whose building blocks are a quantum dot (QD) and a quantum point contact (QPC). This device delivers virtually no power to the electron domain to be measured. We model its operation with standard theory and analyze its performance by choosing realistic parameters. Finally, we discuss the problem of measurement backaction.

An implementation of the QDT is shown in Fig. 1(a). The QD, typically defined by split-gate confinement, is connected by tunnel barriers to two distinct 2DEG regions, one of which is the electron domain to be measured. At zero bias, every time a resonant level of the dot crosses the Fermi energy of the leads, the conductance displays a Coulomb-blockade peak.[11] If the two leads share the same temperature, the latter is simply determined from the peak linewidth, to which it is proportional.[12] On the other hand, when the temperature of the source and drain leads are different, one can still detect the two temperatures independently by applying a voltage bias much greater than the thermal energy of the hotter lead, or even with a single zero-bias measurement, provided the temperature difference is large enough.[13]

Based on a transport measurement, this scheme unavoidably brings in dissipation. Of the total power dissipated during the operation of the thermometer, let us estimate the fraction $\dot{Q}_R$ that goes to the domain. This is associated to the tunneling of hot quasiparticles, contributing a heat flow $\dot{Q}_R = \Gamma E f(E)$, where Γ is the coupling strength between the resonant level of the dot and the domain (assumed to be energy and temperature-independent), E is the energy of the resonant level (with respect to the Fermi energy of the domain), and f is the electron distribution function in the
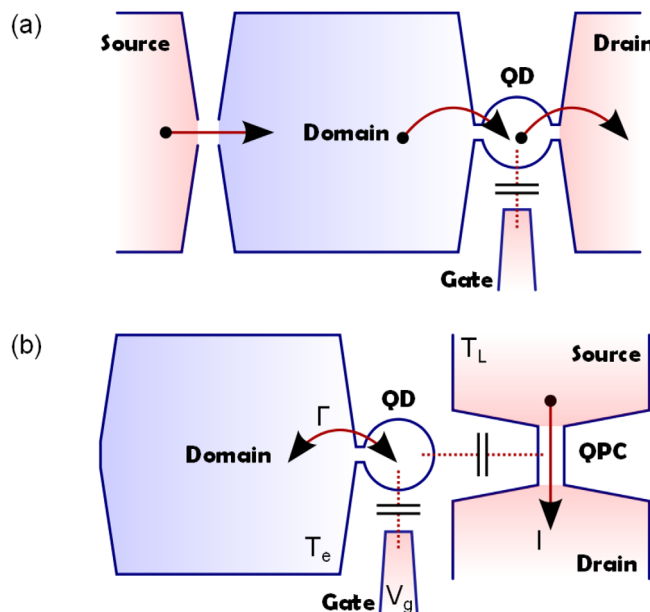

FIG. 1. Galvanic (a) versus nongalvanic (b) QDT. In (a), temperature is determined by the linewidth of Coulomb-blockade peaks, obtained from a transport measurement. In (b), from the average occupation of the dot, read out in a nongalvanic fashion by a QPC placed nearby.

a)Electronic mail: simone.gasparinetti@aalto.fi.

domain. We shall assume that a quasiequilibrium regime[10] holds, so that $f(E) = [1 + \exp(E/k_B T_e)]^{-1}$, T_e being the temperature of the domain.

To perform the readout, we must vary E in a range wide enough to characterize the spread of the Fermi distribution. For definiteness, we set this range to $[-3k_B T_e, 3k_B T_e]$, so that f takes values between 0.05 and 0.95. Averaging over such a sweep, we obtain $\langle \dot{Q}_R \rangle \approx 0.55 \, \Gamma k_B T_e$. Now, a lower bound for Γ comes from the need for adequate signal-to-noise ratio, the current at resonance being of the order of $e\Gamma$. If we set 1 pA as a minimum value, we get $\Gamma > 10$ MHz. On the other hand, Coulomb-blockade thermometry requires thermal broadening of the peak to dominate above intrinsic (Lorentzian) broadening. This condition, which must hold regardless of dissipation, reads $h\Gamma \ll k_B T_e$; for $T_e = 10$ mK, it gives $\Gamma \ll 200$ MHz.

In the following, we will assume $\Gamma = 10$ MHz, which according to our estimate corresponds to $\dot{Q}_R/T_e \approx 80$ aW/K. This figure must be compared to the cooling power provided by all relevant heat-relaxation channels. For definiteness, let us take as the electron domain a portion of a GaAs/AlGaAs 2DEG of representative density and mobility. At subkelvin temperatures, the heat flow from electrons into phonons is given (for GaAs-based 2DEGs) by the expression $\dot{Q}_{e-ph} = \Sigma A(T_e^5 - T_{ph}^5)$,[14] where T_{ph} is the temperature of the phonon bath, A is the area of the domain, and Σ is a constant of the order of 30 fW $\mu m^{-2} K^{-5}$.[13,15]

In Figure 2, we plot the steady-state T_e for 1 and 100 μm^2-sized domains, versus T_{ph}. T_e is determined from a power balance equation of the form $\sum_i \dot{Q}_i[T_e] = 0$, with Q_i denoting the heat flow into the domain due to the ith channel.

Each curve refers to a different configuration, to be discussed below. The straight line marked $T_e = T_{ph}$ is plotted for reference, and stands for the case where no additional heat load is put on the domain. As soon as the QDT is introduced, the situation changes dramatically: T_e follows T_{ph} only down to about 100 mK, below which a saturation occurs. This is due to the weakening of electron-phonon interaction, which is no longer able to carry the dissipated heat away. Furthermore, as $\dot{Q}_{e-ph}$ scales with the domain
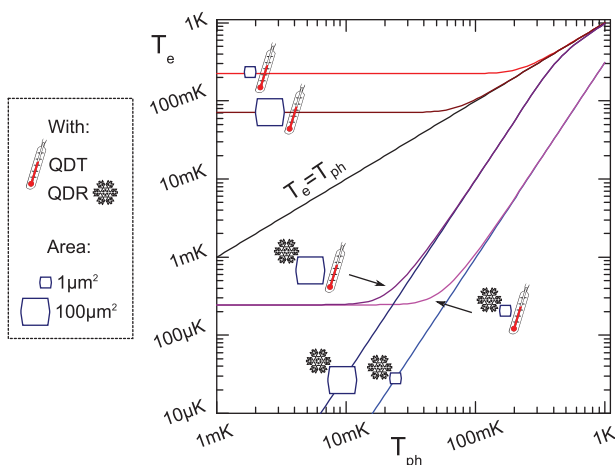
area, the smaller domain saturates at a higher T_e. The ineffectiveness of the electron-phonon coupling at these temperatures has recently motivated the development of electronic coolers.[10,16] We take this possibility into account by considering the case where a quantum-dot refrigerator (QDR)[17–19] is used to cool down the domain, both in the presence and in the absence of the QDT. For simplicity, we assume that the QDR is operated in ideal conditions, so that its cooling power is given by the expression[18] $Q_{QDR} = CT_e^2$, with $C \approx 0.31$ pW/K^2. Thanks to the QDR, the curves with QDT + QDR now saturate at much lower temperatures, of the order of 1mK or below. Notice that the saturating T_e no longer depends on the domain area; this is because at such low temperatures, the competition is between the QDT and the QDR, with the phonon bath playing little or no role. For simplicity, in the discussion above, we have included no other sources of heat besides the QDT. In reality, the electronic temperature is eventually limited by parasitic heat sources, such as radiation from higher-temperature stages and noise in the electrical lines. Likewise, the performance assumed for the QDR must be taken as an idealization: a recent experiment[19] pointed out deviations from the ideal behavior already at 110mK, possibly due to nonequilibrium effects.

The nongalvanic device that we propose is shown in Fig. 1(b). As in the QDT discussed above, the strongly nonlinear density of states of a QD is exploited to probe the energy distribution of the domain. All the difference lies in the way this information is read out: instead of performing a transport measurement across the dot, we measure its average occupation in a nongalvanic fashion with the help of a QPC placed nearby.[20–22] If the gate sweep is performed adiabatically, the heat flow into the domain is minimal, making the nongalvanic thermometer a candidate device for temperature measurements of ultracold electron domains. In the following, we will describe its operation with a quantitative model.

Let us start from the QD. The latter is preferably operated in the "quantum" Coulomb blockade regime, meaning that both its charging energy and orbital level spacing are much greater than the thermal energy. As a result, electron tunneling only takes place between the dot and a single energy level. As for the galvanic QDT, we further require $h\Gamma \ll k_B T_e$, so that we can neglect intrinsic broadening effects. The mean occupation of the level is then given by

$$\langle n_{dot} \rangle = f(E_0^{QD} - e\alpha V_G), \tag{1}$$

where E_0^{QD} is a reference energy for the level and α the lever arm of the gate on the dot.

Our next question is how the change in $\langle n_{dot} \rangle$ affects the current I through the QPC, in the presence of a voltage bias V_b. In the Landauer-Büttiker formalism,[23] $I = \frac{2e}{h} \int_{-\infty}^{\infty} dE \mathcal{T}(E, E^{QPC})[f(E - eV_b, T_L) - f(E, T_L)]$, where T_L is the temperature of the QPC leads (in general, $T_e \neq T_L$) and $\mathcal{T}(E, E^{QPC})$ is the energy-dependent transmission coefficient of the QPC. Assuming a single ballistic channel and using a saddle potential,[24] $\mathcal{T}(E, E^{QPC}) = \{1 + \exp[-2\pi(E - E^{QPC})/\hbar\omega_x]\}^{-1}$, where ω_x is a characteristic energy of the confinement and E^{QPC} denotes the bottom of the potential for the one-dimensional electron channel defined by the QPC. Upon
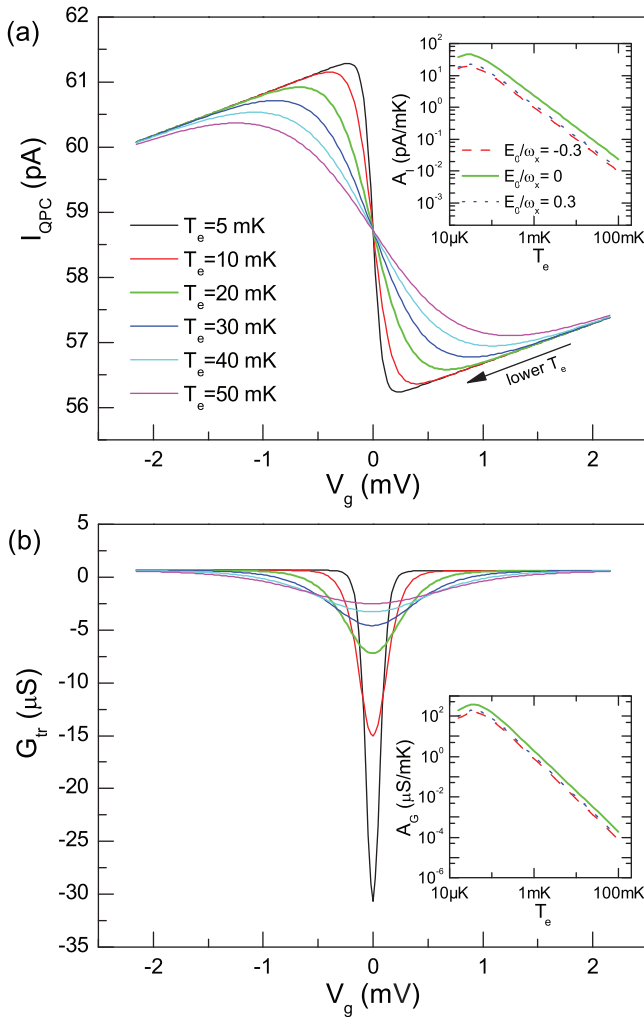
FIG. 2. Steady-state electron temperature T_e versus phonon bath temperature T_{ph}, for domains of different areas, in the presence of a QDT, a QDR, or both. Parasitic heat loads on the system are not taken into account.

FIG. 3. (a) QPC current I versus gate voltage V_g for different values of the domain temperature T_e; a steeper sawtooth corresponds to a lower T_e. Inset: current gain A_I versus T_e for three different QPC working points. (b) Transconductance G_{tr} versus V_G for the same set of temperatures as in (a); a sharper peak corresponds to a lower T_e. Inset: Transconductance gain A_G versus T_e [same working points as in (a)]. Parameters: $T_L = 20$ mK, $\omega_x = 1$meV, $E_C = 2$K, $\beta = 0.1$, $\alpha = 0.01$, $\gamma = 0.002$. In the main panels, $E_0/\omega_x = -0.3$. In the insets, the gains are evaluated at optimal V_g points. For A_I, we take into account 1 μV fluctuations of V_g. For A_G, the curves are those expected for a lock-in measurement with 1 μV signal amplitude.

changing V_g, the potential landscape at the QPC changes due to the capacitive couplings QPC-QD and QPC-gate. As these couplings are small, we regard them as perturbations and model their effect by a shift of the potential E^{QPC} with respect to a reference value E_0^{QPC}. The latter is tuned by the gates defining the constriction and defines the working point of the QPC. We shall further denote by β the lever arm of the dot on the QPC, and by γ that of the gate. In general, we expect $\gamma \ll \beta$. Then we write E^{QPC} as

$$E^{QPC} = \beta \frac{e^2 \langle n_{dot} \rangle}{C_\Sigma} - e\gamma V_G - E_0^{QPC}. \qquad (2)$$

In the limit $eV_b, k_B T_L \ll \hbar\omega_x$, $\mathcal{T}$ is approximately constant in the range where the electron distributions of the leads vary. The expression for I then simplifies as $I = \frac{2e^2}{h}\mathcal{T}(0, E^{QPC})V_b$. Notice that T_L no longer appears in this expression. By contrast, T_e determines $\langle n_{dot} \rangle$, which affects E^{QPC} and hence $\mathcal{T}$.

In Fig. 3(a), we plot I versus V_g for different values of T_e. As V_g is made more negative, I steadily decreases due to the spurious coupling between the gate and the QPC. Yet as the resonant level crosses the Fermi energy of the domain from above, $\langle n_{dot} \rangle$ sharply decreases by one, leading to a step-like increase in I. This gives rise to a sawtooth pattern at zero temperature, which gets progressively smeared as T_e is increased.

Besides I, a relevant quantity for thermometry is the gate-to-QPC transconductance $G_{tr} = dI/dV_g$, which can be directly measured using a lock-in amplifier. By direct calculation, we find

$$G_{tr} = \frac{2e^2}{h}eV_b\frac{d\mathcal{T}}{dE^{QPC}}\left(\gamma + \alpha\beta\frac{e^2}{C_\Sigma}\frac{df}{dE}\right). \qquad (3)$$

As a function of V_g, a series of dips appear on top of a positive baseline [see Fig. 3(b)]. The dips are proportional to the derivative of the Fermi function, and their FWHM ΔV_g to the domain temperature T_e. Explicitly,

$$T_e = \frac{e\alpha}{2\log(3 + 2\sqrt{2})k_B}\Delta V_g. \qquad (4)$$

The constant relating ΔV_g to T_e is a simple combination of fundamental constants and the lever arm α, which can be determined experimentally from a measurement of the QD charging energy and the cross-capacitance between the gate and the QD. This fact makes of the nongalvanic QDT a primary thermometer, i.e., a thermometer that can measure absolute temperatures without relying on other thermometers (e.g., for calibration).[10]

We conclude this discussion by giving a figure of merit for each measurement mode. If we choose to measure I, such a figure may well be the current gain $A_I = \delta I/\delta T_e$, the ratio being taken at the gate position V_g^{opt} that maximizes it. In the inset of Fig. 3(a), A_I is plotted versus T_e over a broad range of temperatures and for different QPC working points. The maximum gain is obtained by choosing $E_0^{QPC} = 0$, which corresponds to $\mathcal{T} = \frac{1}{2}$. At 100 μK, it can exceed 10 pA/mK. Since A_I scales as the inverse of T_e, the lower the temperature, the higher the gain. Yet, the sharpness of the sawtooth also increases at lower temperature, so that the measurement becomes more and more sensitive to the dot potential. Fluctuations of V_g of the order of 1 μV, included in the model, are responsible for the bending of the curves below 50 μK. As for G_{tr}, we can proceed in the same way and define a transconductance gain $A_G = \delta G_{tr}/\delta T_e$. A_G is plotted in the inset of Fig. 3(b). Similarly to A_I, A_G is also maximized when $\mathcal{T} = \frac{1}{2}$. At 100 μK, $A_G \approx 100$ μS/mK. The dependence on T_e is the same as for A_I. At very low T_e, A_G is eventually limited by the amplitude of the lock-in modulation applied to V_g.

So far, we have implicitly assumed that the state of the QD is not influenced by our readout procedure; that is, we have neglected any measurement backaction. In the following, we shall take it into account and show that its effects are indeed negligible in a suitable range of parameters. In doing so, we are led to consider two different mechanisms: current fluctuations through the QPC (that is, shot noise)[25–28] and charge fluctuations in the QPC (Refs. 29 and 30). The nature of these two is very different. In particular, the way current

fluctuations couple to the dot depends on the specific measurement circuit. By contrast, the backaction due to charge fluctuations is fundamentally unavoidable. Indeed, it is related to the Heisenberg backaction of the detector (QPC) on the quantum system whose state we are measuring (QD).[30]

We shall describe both mechanisms using the theory of photon-assisted tunneling (PAT).[31] Let $S_V(\omega)$ be the spectrum of voltage fluctuations on the dot; the probability of PAT with energy E is then $P(E) = \frac{1}{h}\int_{-\infty}^{\infty}\exp\left[J(t) + i\frac{E}{\hbar}t\right]dt$, where the phase-phase correlation function $J(t)$ is related to $S_V(\omega)$ by $J(t) = \frac{2\pi}{\hbar R_K}\int_{-\infty}^{\infty}\frac{S_V(\omega)}{\omega^2}(e^{-i\omega t} - 1)d\omega$. The modified $\langle n_{dot}\rangle$, accounting for PAT, is given by

$$\langle n_{dot}\rangle = \int_{-\infty}^{\infty} f(E - E_0^{QD} - e\alpha V_G)P(E)dE, \qquad (5)$$

which is a convolution of the distribution function of the domain with the $P(E)$ function. Even in the presence of PAT, our previous analysis is still correct provided $P(E)$ is cutoff at some energy $\bar{E} \ll k_B T$, for in that case, we can approximate $P(E) \approx \delta(E)$ and recover the unperturbed result.

Let us consider current noise first. Given its spectral density $S_I(\omega)$, the spectrum of voltage fluctuations in the dot is obtained by $S_V(\omega) = |Z(\omega)|^2 S_I(\omega)$, where we have introduced a transimpedance Z as in Ref. 32. As a first approximation, we may write $Z(\omega) \approx Z(0) = \tau R_S$, where R_S is the resistance of the QPC leads and τ is a lever arm describing the asymmetric coupling between QD and QPC leads. The behavior of $P(E)$ at finite energies is then given by $P(E) = \frac{2\pi}{R_K}\frac{Z^2 S_I(E/\hbar)}{E^2}$, where $R_K = h/2e^2$ is the resistance quantum. Taking normalization into account, we find that the energy spread of $P(E)$ is of the order of $\bar{E} = Z^2 S_I/R_K$. Now, shot noise in the QPC has the spectrum[25] $S_I = (eV_b/R_K)\mathcal{T}(1 - \mathcal{T})$. If we take $R_S = 0.1R_K$, $\tau = 0.1$, $\mathcal{T} = 1/2$ and $V_b = 2.5\,\mu\text{V}$ (so that $I = 100\,\text{pA}$), we get $\bar{E}/k_B = 3\,\mu\text{K}$. As revealed by this analysis, the backaction due to current noise can be made negligible by a combination of low-resistance leads and small V_b.

Let us now turn to charge noise. The spectrum of charge fluctuations on the dot, induced by the QPC, is given to the first order in V_b and ω by the expression $S_Q(\omega) = 2C_\mu^2 R_v eV_b$, where R_v is the nonequilibrium charge relaxation resistance defined in Ref. 29, and C_μ the electrochemical capacitance of the QPC "to" the dot. Charge fluctuations are related to voltage fluctuations by the total capacitance of the dot: $S_V = (1/C_\Sigma)^2 S_Q$, so that $S_V = 2(C_\mu/C_\Sigma)^2 eV_b R_v$. As for current noise, we have $P(E) = \frac{2\pi}{R_K}\frac{S_V(E/\hbar)}{E^2}$. The energy spread for this $P(E)$ is given by $\bar{E} = (C_\mu/C_\Sigma)^2(R_v/R_K)eV_b$. We estimate its magnitude by taking $C_\mu/C_\Sigma = 0.02$, $R_v = 0.1R_K$, $V_b = 2.5\,\mu\text{V}$. We get $\bar{E}/k_B \approx 1\,\mu\text{K}$, implying that we can safely neglect charge noise down to very low temperatures. This primarily stems from the ratio C_μ/C_Σ being very small, as typical for split-gate-defined nanostructures. In addition, the same prescription as for current noise must be applied to V_b.

In conclusion, we have addressed the problem of measuring the temperature of 2DEG microdomains cooled down to the base temperature of state-of-art dilution refrigerators and possibly below. Already at 100 mK, conventional schemes based on transport are inadequate, due to overheating. We have argued that nongalvanic thermometry may overcome this limitation. Our results suggest that a nongalvanic thermometer such as that considered may be conveniently employed at temperatures ranging from tens of mK down to tens of μK.

[1]T. Ando, B. Fowler, and F. Stern, Rev. Mod. Phys. **54**, 437 (1982).

[2]W. Pan, J. Xia, V. Shvarts, D. E. Adams, H. L. Stormer, D. C. Tsui, L. N. Pfeiffer, K. W. Baldwin, and K. W. West, Phys. Rev. Lett. **83**, 3530 (1999).

[3]A. C. Clark, K. K. Schwarzwälder, T. Bandi, D. Maradan, and D. M. Zumbühl, Rev. Sci. Instr. **81**, 103904 (2010).

[4]Y. Ji, Y. Chung, D. Sprinzak, M. Heiblum, and D. Mahalu, Nature **422**, 415 (2003).

[5]P. Simon and D. Loss, Phys. Rev. Lett. **98**, 156401 (2007).

[6]R. M. Potok, I. G. Rau, H. Shtrikman, Y. Oreg, and D. Goldhaber-Gordon, Nature **446**, 167 (2007).

[7]S. P. Giblin, S. J. Wright, J. D. Fletcher, M. Kataoka, M. Pepper, T. J. B. M. Janssen, D. A. Ritchie, C. A. Nicoll, D. Anderson, and G. A. C. Jones, New J. Phys. **12**, 073013 (2010).

[8]R. Hanson, L. P. Kouwenhoven, J. Petta, S. Tarucha, and L. M. K. Vandersypen, Rev. Mod. Phys. **79**, 1217 (2007).

[9]C. Nayak, A. Stern, M. Freedman, and S. Das Sarma, Rev. Mod. Phys. **80**, 1083 (2008).

[10]F. Giazotto, T. T. Heikkilä, A. Luukanen, A. M. Savin, and J. P. Pekola, Rev. Mod. Phys. **78**, 217 (2006), and references therein.

[11]C. W. J. Beenakker, Phys. Rev. B **44**, 1646 (1991).

[12]L. P. Kouwenhoven, C. M. Marcus, P. L. McEuen, S. Tarucha, R. Westervelt, and N. S. Wingreen, "Electron transport in quantum dots," in *Mesoscopic Electron Transport*, edited by L. L. Sohn, L. P. Kouwenhoven, and G. Schön (Kluwer, 1997), pp. 16–23.

[13]S. Gasparinetti, F. Deon, G. Biasiol, L. Sorba, F. Beltram, and F. Giazotto, Phys. Rev. B **83**, 201306(R) (2011).

[14]P. Price, J. Appl. Phys. **53**, 6863 (1982).

[15]N. J. Appleyard, J. T. Nicholls, M. Y. Simmons, W. R. Tribe, and M. Pepper, Phys. Rev. Lett. **81**, 3491 (1998).

[16]J. T. Muhonen, M. Meschke, and J. P. Pekola, Rep. Prog. Phys. **75**, 046501 (2012).

[17]H. L. Edwards, Q. Niu, and A. L. de Lozanne, Appl. Phys. Lett. **63**, 1815 (1993).

[18]H. L. Edwards, Q. Niu, G. A. Georgakis, and A. L. de Lozanne, Phys. Rev. B **52**, 5714 (1995).

[19]J. R. Prance, C. G. Smith, J. P. Griffiths, S. J. Chorley, D. Anderson, G. A. C. Jones, I. Farrer, and D. A. Ritchie, Phys. Rev. Lett. **102**, 146602 (2009).

[20]M. Field, C. G. Smith, M. Pepper, D. A. Ritchie, J. E. F. Frost, G. A. C. Jones, and D. G. Hasko, Phys. Rev. Lett. **70**, 1311 (1993).

[21]J. M. Elzerman, R. Hanson, L. H. Willems van Beveren, B. Witkamp, L. M. K. Vandersypen, and L. P. Kouwenhoven, Nature **430**, 431 (2004).

[22]The principle of nongalvanic thermometry may as well be applied to metallic systems, with a single-electron transistor playing the role of the QPC, as in O.-P. Saira, A. Kemppinen, V. Maisi, and J. Pekola, Phys. Rev. B **85**, 012504 (2012).

[23]R. Landauer, IBM J. Res. Dev. **32**, 306 (1988).

[24]M. Büttiker, Phys. Rev. B **41**, 7906 (1990).

[25]Y. Blanter and M. Büttiker, Phys. Rep. **336**, 1 (2000).

[26]E. Onac, F. Balestro, L. H. W. van Beveren, U. Hartmann, Y. V. Nazarov, and L. P. Kouwenhoven, Phys. Rev. Lett. **96**, 176601 (2006).

[27]S. Gustavsson, M. Studer, R. Leturcq, T. Ihn, K. Ensslin, D. Driscoll, and A. Gossard, Phys. Rev. Lett. **99**, 206804 (2007).

[28]S. Gustavsson, I. Shorubalko, R. Leturcq, T. Ihn, K. Ensslin, and S. Schön, Phys. Rev. B **78**, 035324 (2008).

[29]M. Pedersen, S. A. Van Langen, and M. Büttiker, Phys. Rev. B **57**, 1838 (1998).

[30]C. E. Young and A. A. Clerk, Phys. Rev. Lett. **104**, 186803 (2010).

[31]G. Ingold and Y. V. Nazarov, "Charge tunneling rates in ultrasmall junctions," in *Single Charge Tunneling*, edited by H. Grabert and M. H. Devoret (Plenum, New York, 1992), Vol. 294, Chap. 2, pp. 21–107.

[32]R. Aguado and L. Kouwenhoven, Phys. Rev. Lett. **84**, 1986 (2000).